Cell Reports, Volume *43*

Supplemental information

The *Cryptosporidium* signaling kinase CDPK5 plays an important role in male gametogenesis and parasite virulence

Maria G. Nava, Joanna Szewczyk, Justine V. Arrington, Tauqeer Alam, and Sumiti Vinayak

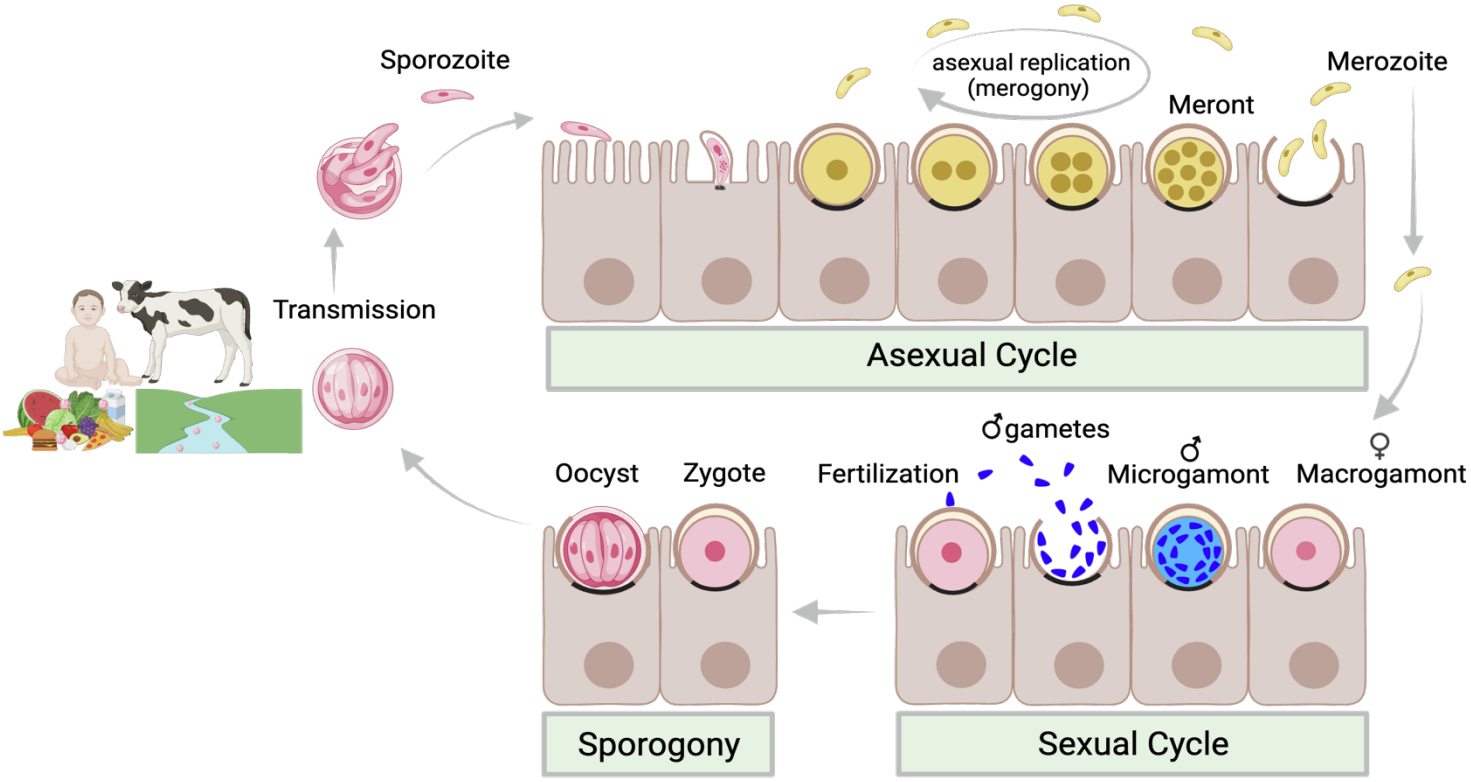

Figure S1. Life cycle of *Cryptosporidium*. Created with BioRender.com

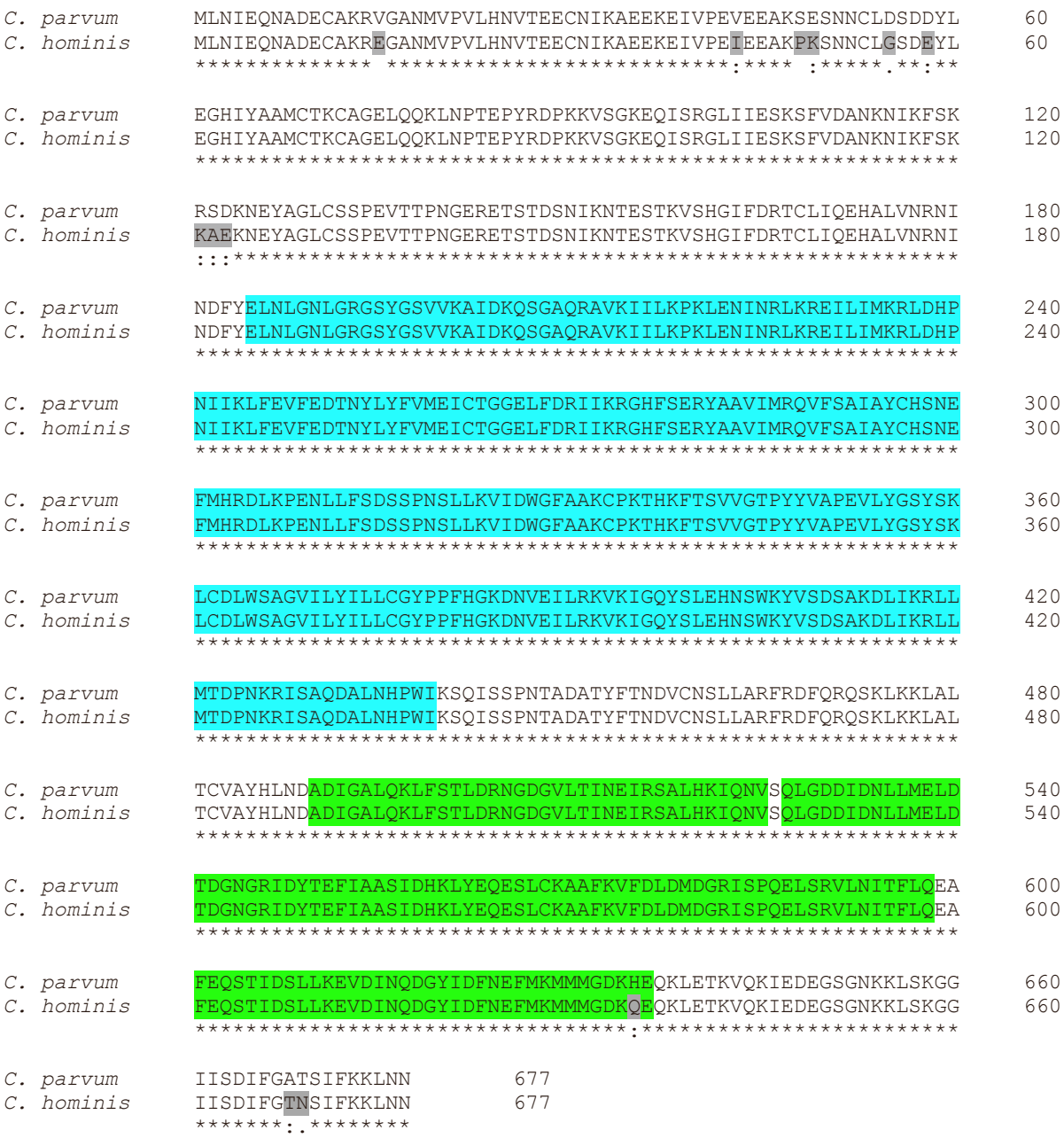

Figure S2. Amino acid alignment of CDPK5 from *C. parvum* (N=158) and *C. hominis* (N=96) isolates. Alpha-fold prediction of protein domains, serine-threonine kinase catalytic domain (185-439 amino acids) and EF-hand calcium binding domains (490-525, 527-562, 563-598, 601-636 amino acids) are shaded in blue and green, respectively. Amino acid changes between *C. parvum* and *C. hominis* are highlighted in gray.

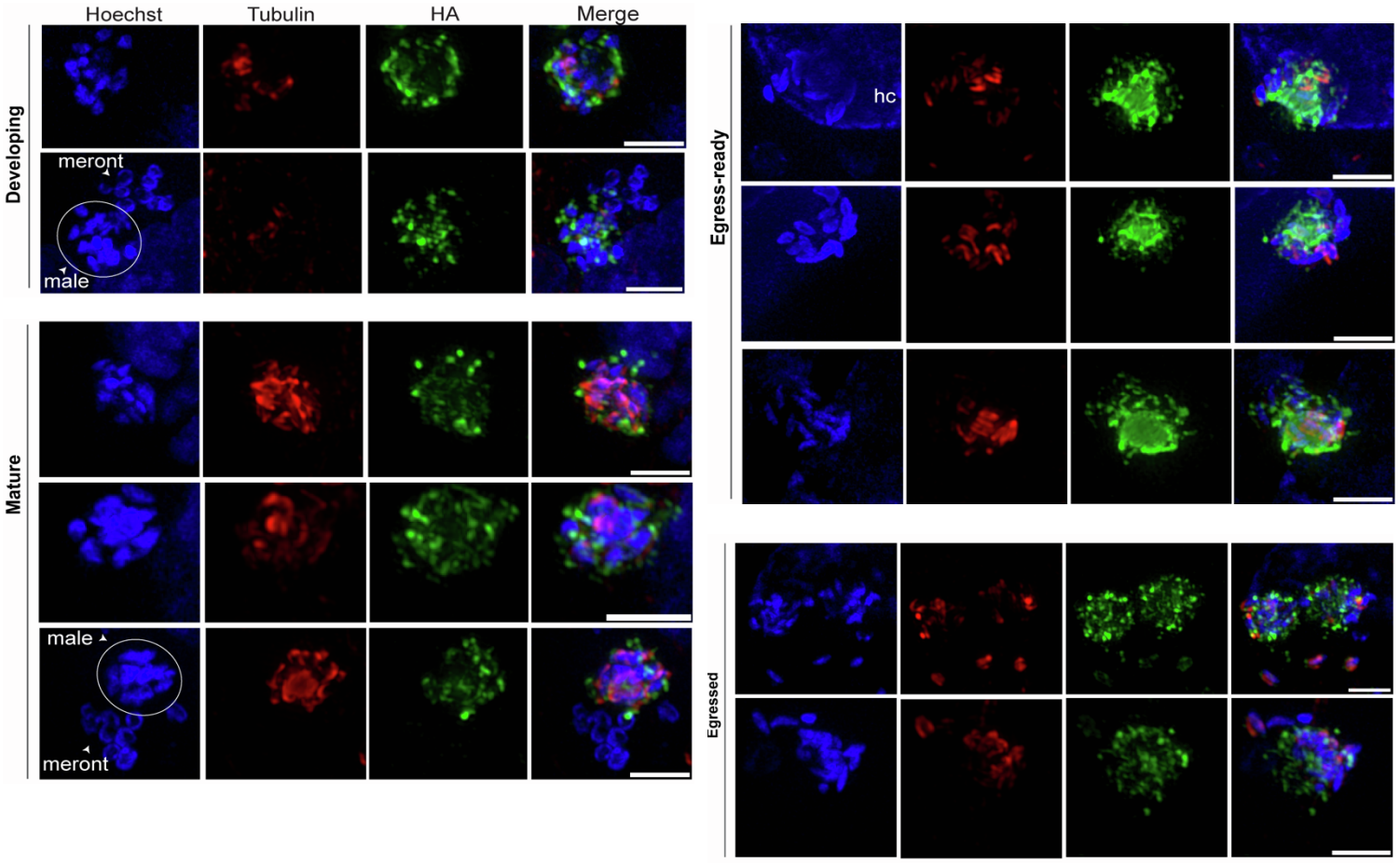

Figure S3. **Additional super-resolution images of CDPK5 localization during male gametogenesis.** Developing, mature, egress-ready, and egressed stages are shown. Anti-HA (green), anti-alpha-tub (tub, red) antibodies and Hoechst staining of parasite nuclei (blue) were used to follow gamont development. hc, host cell. No HA staining was seen in meronts captured in the same field. Scale bars, 2 μm. Data from three technical replicates and three independent experiments are shown.

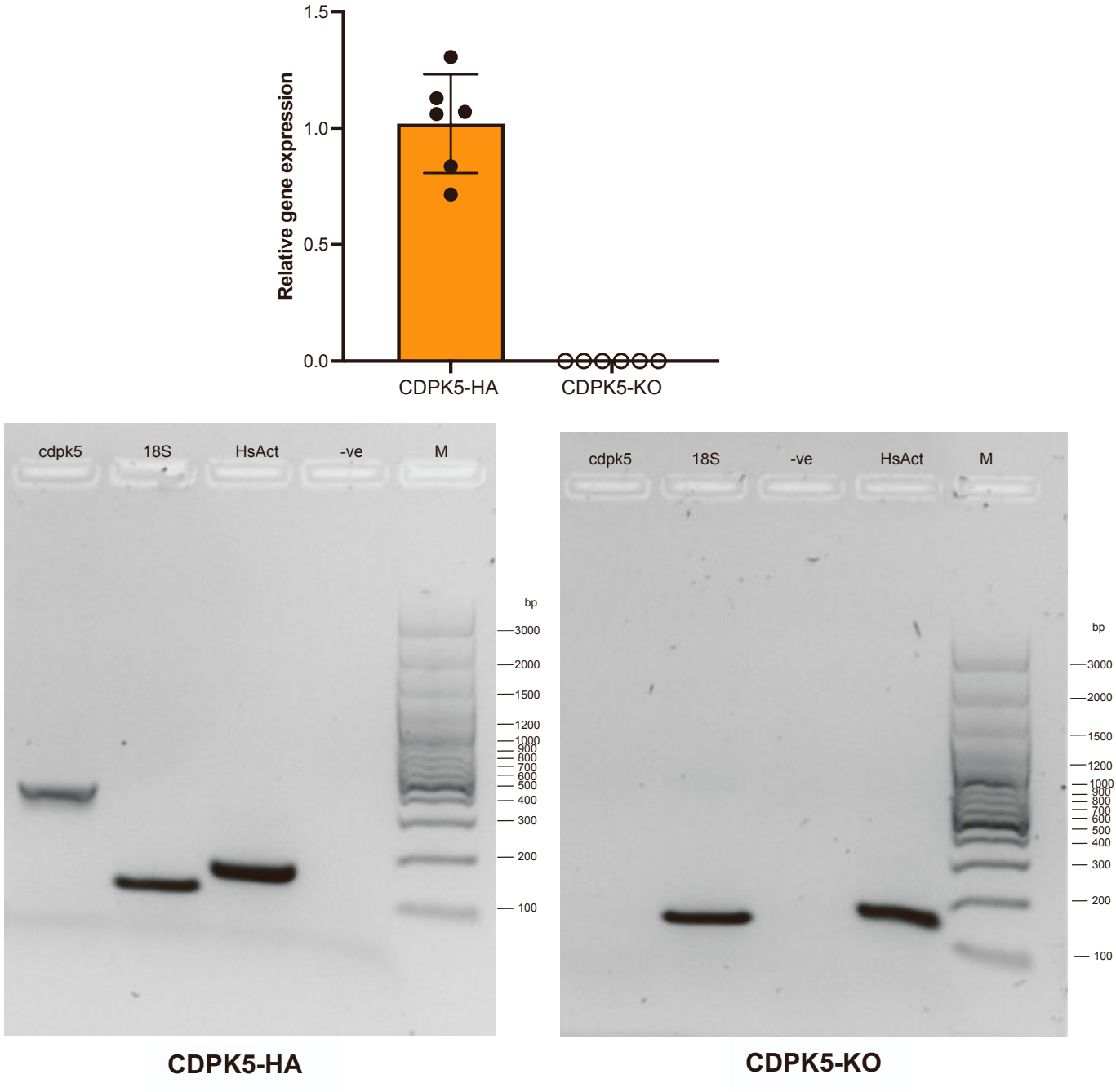

Figure S4. qRT-PCR and representative gel showing lack of *C. parvum cdpk5* gene expression in CDPK5-KO transgenic, while expression is seen in the CDPK5-HA transgenic at 48 hours p.i of HCT-8 cells. qPCR products were subjected to agarose gel electrophoresis and no band for the *cdpk5* gene was seen in CDPK5-KO, while it was seen for CDPK5-HA transgenic. cdpk5, *cdpk5* gene (416 bp); 18S, 18S rRNA (159 bp); HsAct, Human Actin (194 bp); -ve, negative control. Inverted gel images are shown. Primer sequences are provided in Table S2. For qPCR, data points are mean ± SD from six technical replicates.

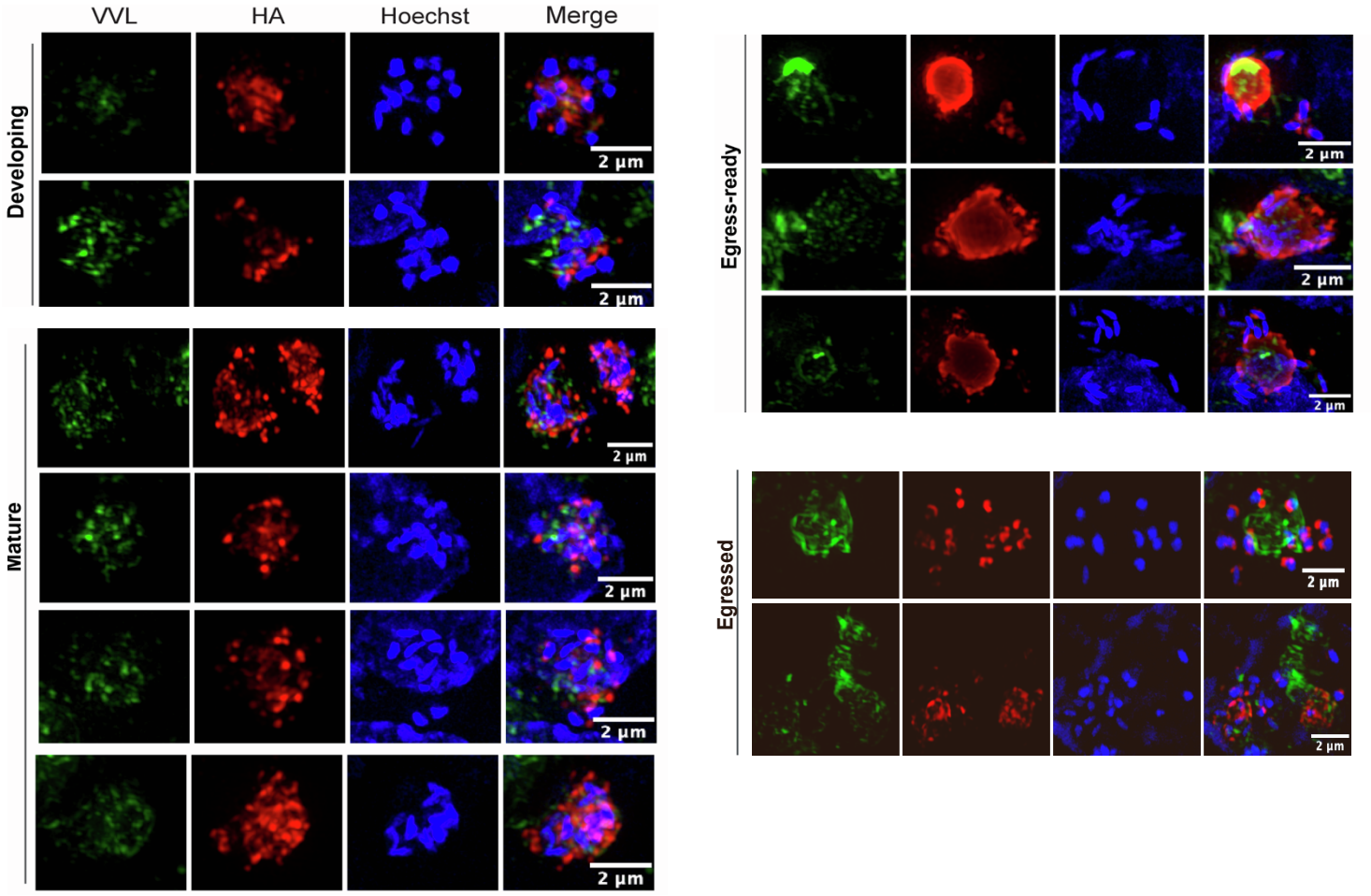

Figure S5. **Additional representative super-resolution images of CDPK5-HA transgenic parasites showing localization of CDPK5 during different stages of male gametogenesis.** Developing, mature, egress-ready, and egressed stages are shown. VVL (green), HA (red) and nuclear staining (blue) were used to identify and categorize stages. Scale bars, 2 µm. Data shown here are from three technical replicates and two independent experiments.

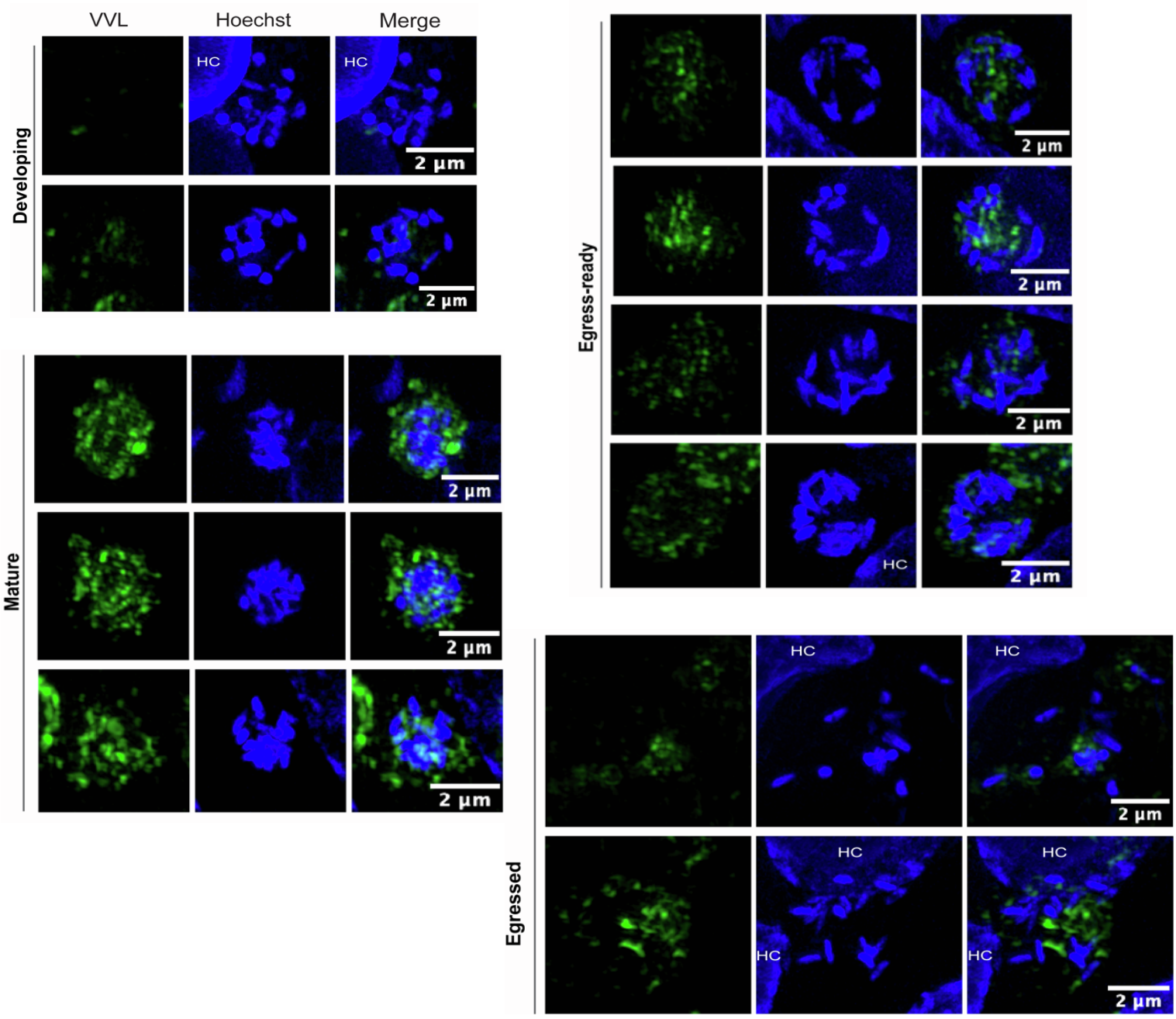

Figure S6. **Additional representative images of CDPK5-KO transgenic parasites showing localization of CDPK5 during different stages of male gametogenesis**. Developing, mature, egress-ready, and egressed stages are shown. VVL (green) and nuclear staining (blue) were used to identify and categorize stages. HC, Host cell nucleus. Scale bars, 2 µm. Data shown here are from three technical replicates and two independent experiments.

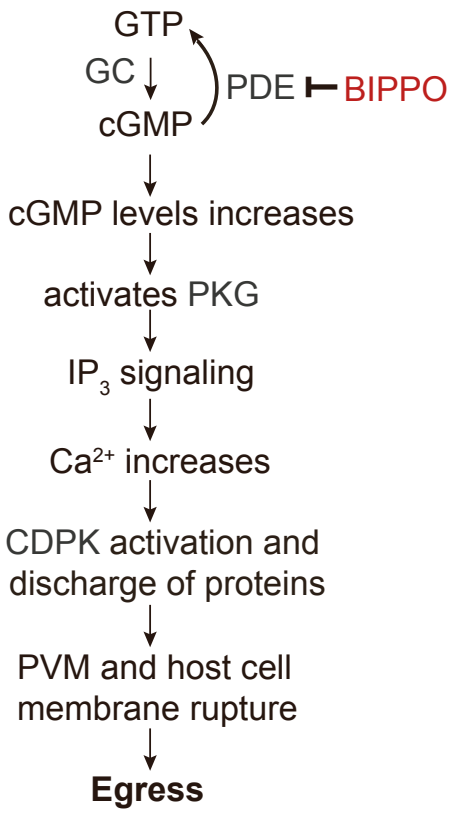

Figure S7. **Diagram showing known signaling events in *Plasmodium* and *Toxoplasma* that lead to zoite egress.** 3′, 5′-cyclic guanosine monophosphate, cyclic GMP; GC, guanylyl cyclase; PDE, 3′,5′-cyclic nucleotide phosphodiesterase; BIPPO (PDE inhibitor), benzyl-3-isopropyl-1Hpyrazolo[4,3-d] pyrimidin-7(6H)-one; PKG, cGMP-dependent protein kinase G; IP_3, inositol 1,4,5-trisphosphate signaling; PVM, parasitophorous vacuole membrane.

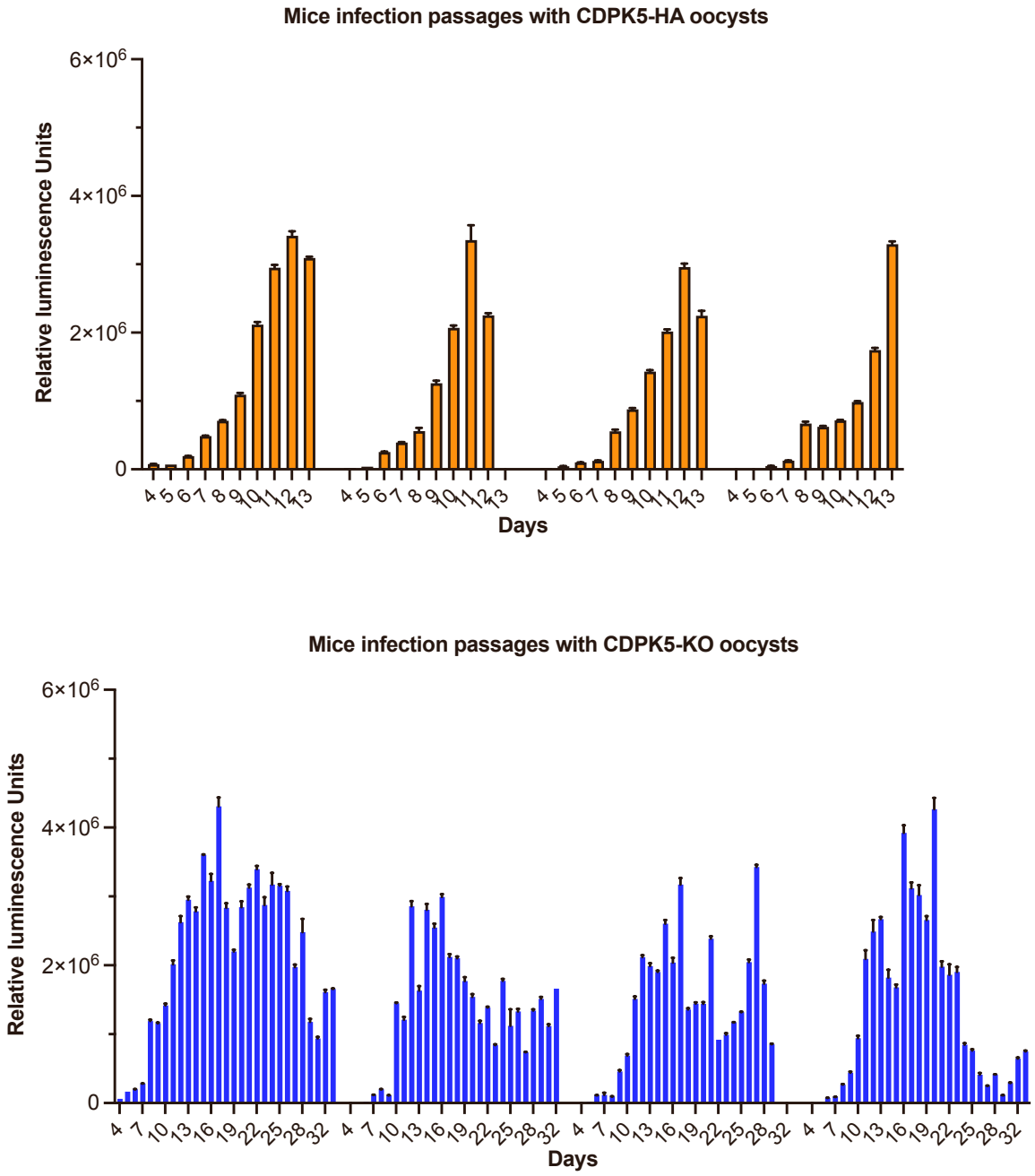

Figure S8. Multiple passages of transgenic oocysts into IFN-γ KO mice show similar infection dynamics, with no loss in infectivity potential. Fecal luminescence measurements of mice infected with 5000 purified oocysts. N=5 mice per group were infected for each passage. Luminescence data (mean ± SD) from three technical replicates are shown.

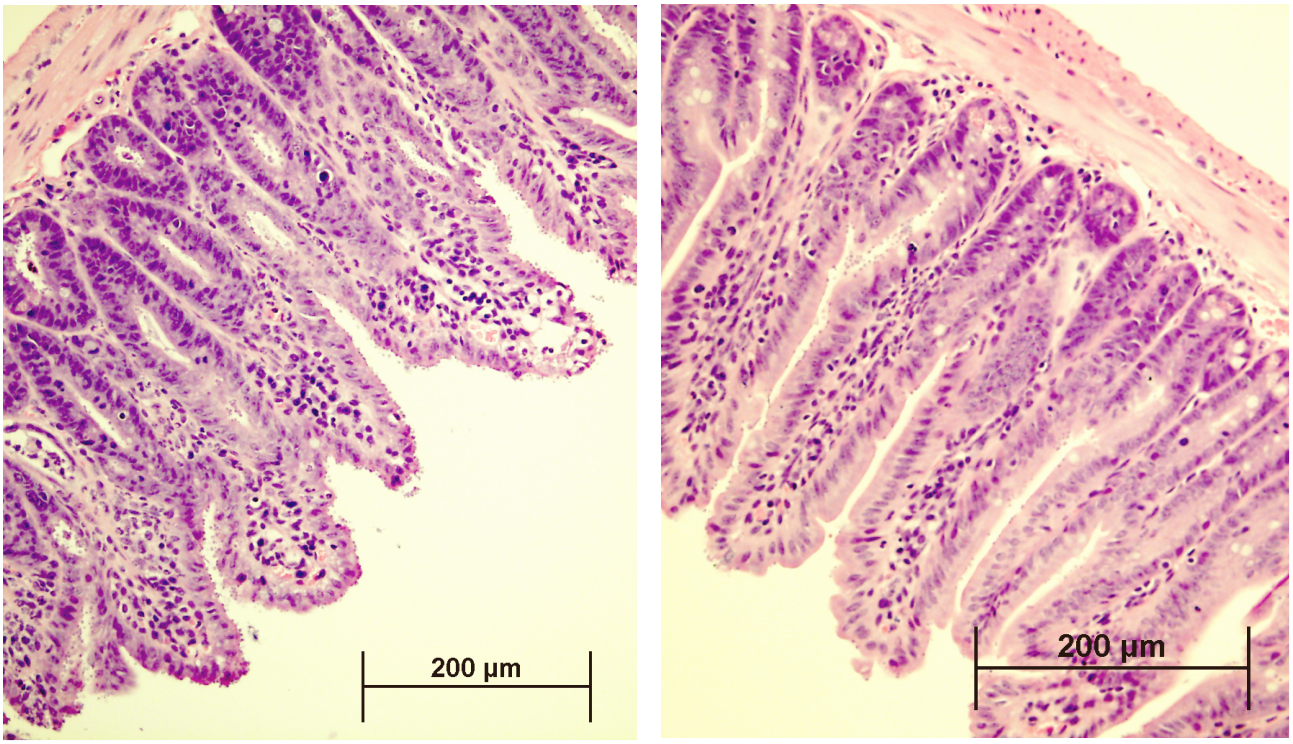

Figure S9. Histology of the small intestine (distal part) from IFN-γ KO mice infected with transgenic *C. parvum* strains. A heavy parasite burden and loss of intestinal architecture is observed in tissue sections from mice infected with CDPK5-HA compared to CDPK5-KO parasites. N=3 mice per group, each mouse was infected with 5000 transgenic oocysts. Scale bars, 200 µm.